Conference Proceedings

EuroSun 2016
Palma de Mallorca (Spain), 11 – 14 October 2016

Modelling clear sky DNI under extreme aerosol loading: the case of Saharan outbreak in south-east Spain

Joaquín Alonso-Montesinos[1, 2], Jesús Polo[3], Gabriel López[4], Javier Barbero[1], Juan Luis Bosch[4], Jesús Ballestrín[5] and Francisco Javier Batlles[1, 2]

[1] Department of Chemistry and Physics, University of Almería, 04120 Almería, Spain

[2] CIESOL, Joint Centre University of Almería-CIEMAT, 04120 Almería, Spain

[3] Photovoltaic Solar Energy Unit (Renewable Energy Division, CIEMAT), 28040 Madrid, Spain

[4] Department of Electrical and Thermal Engineering, Design and Projects, University of Huelva, 21004, Huelva, Spain

[5] Concentrating Solar System Unit (Plataforma Solar de Almería, CIEMAT), 04200 Almería, Spain

Abstract

In this work we analyze the impact of a strong Saharan dust intrusion on the DNI registered at two sites in the southeast of Spain: University of Almería (UAL) and Almería Solar Platform (PSA) located in Tabernas (Almería). Direct normal irradiance (DNI) modelling with ESRA procedure presents high Linke turbidity values, being extremely high at the first site. DNI simulations using SMARTS code in the PSA emplacement, using AERONET data from PSA and maximum desert aerosol type, show a great accordance with the measured DNI values. In the UAL emplacement, SMARTS simulation of DNI values seems also to be compatible with maximum desert aerosol type aerosols. Visibility values are in good accordance with the extinction coefficients derived from the CL51 ceilometer profiles.

Keywords: *Aerosol optical depth, solar irradiance estimation, DNI simulation, atmospheric attenuation*

1. Introduction

On 21st and 22nd February 2016, an intense episode of Saharan dust intrusion took place in almost all of the Iberian Peninsula, reducing drastically the visibility and producing a remarkable dust deposition. Southeast, where the University of Almería (UAL) and the Almería Solar Platform (PSA) are located, was particularly affected by the event. Fig. 1 shows that relevant entrance of dust in the coast of Almeria region.

doi:10.18086/eurosun.2016.09.10 Available at http://proceedings.ises.org

Fig. 1: MODIS satellite image for Almeria and surroundings on 22nd February 2016. Blue circle denotes PSA site. Red circle, the UAL site.

Observing the previous image, an evidence mineral dust load comes from the south, reaching a higher concentration of dust particles in the coast than in the PSA site. This feature can be also seen in the next image, where the sun reaches a heliostat and the sun's reflection is attenuated gradually due to the presence of concentrated Saharan dust.

Fig. 2: This figure shows the low visibility and the light scattered by the large particles in the atmosphere on 22nd February 2016 at 14:30 in PSA. Solar radiation reflected by the heliostats is attenuated by scattering.

Other African-dust episodes reaching Europe, even at high latitudes have been described so far (Kambezidis et al, 2012). 22nd February was a clear day, almost from sunrise to 14:00 h (when some high clouds appeared, affecting the DNI measurements), and this work analyzes the influence of the high turbidity on the DNI values for both sites. Figure 3 shows the HYSPLIT predicted back-trajectories for the studied area. The HYSPLIT model results corroborate the evidence of an air mass with coarse aerosols particles that enters the Iberian Peninsula from the Sahara desert.

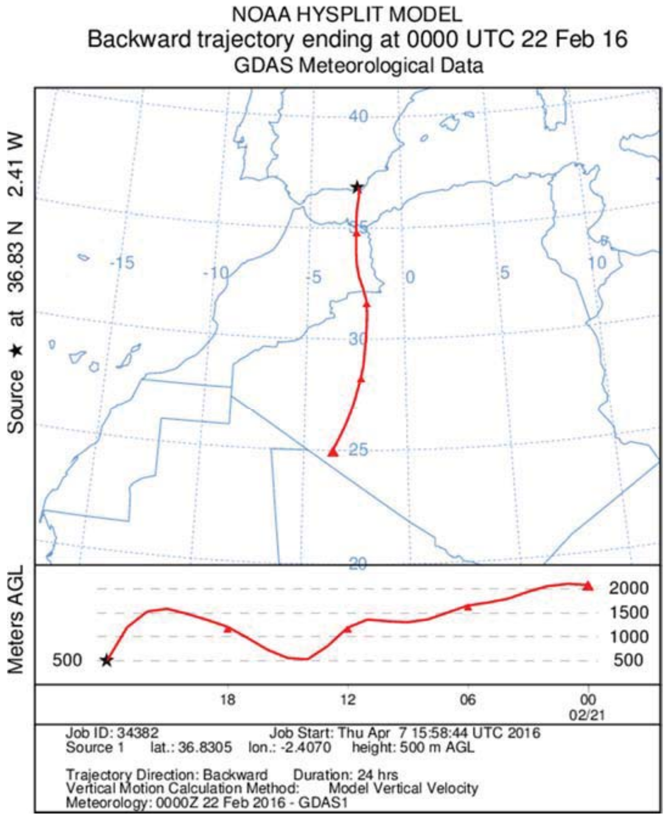

Fig. 3: HYSPLIT back trajectories

2. Data

DNI was measured at UAL station (36.8304º N, 2.4071º W, 0 m above sea level (ASL)), whereas, measurements at PSA (37.0949º N, 2.3614ºW, 550 m ASL) comprised both DNI and aerosol optical thickness (AOT) from the AERONET station.

Figure 4 shows the DNI ground measurements registered during 22nd February in both sites.

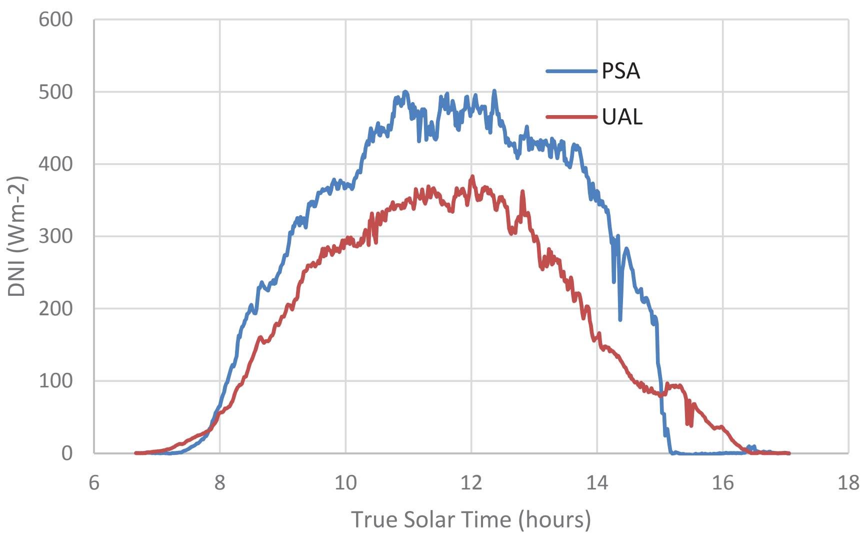

Fig. 4: DNI from PSA and UAL on 22nd February 2016

DNI values show that the daily profiles do not correspond to a clear sky situation for the whole day. After noon there is a clear decrease in DNI not related with an increase of dust concentration (as showed in Figure 4); when upper clouds appeared in the atmosphere. Figure 5 shows the presence of clouds in the solar area and in the surroundings at 16:00 True Solar Time (TST).

Fig. 5: Total sky image on 22nd February 2016 at 16:00 TST

In Figure 6, we show the evolution along the whole day 22nd of the attenuated backscatter intensity (ABI) profiles from ground up to 4 km registered by a CL51 ceilometer (Vaisala), located at the UAL.

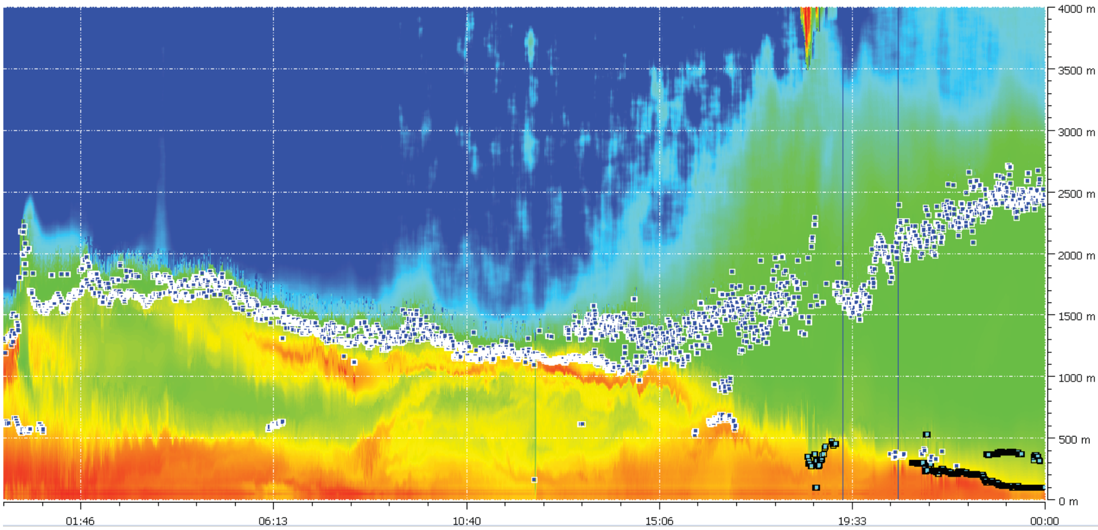

Fig. 6: Attenuated backscatter profiles from CL51 ceilometer at Almeria University

In this figure we observe:

- A nearly static dust layer 500 m thick from the previous day and through sunrise. As the surface temperature rises, this layer expands into the boundary layer.
- Another thin layer, in the upper limit of the residual boundary layer of the previous day, floating on the day 22nd boundary layer. Both layers together, progressively precipitate from 16:00 h through the end of the day.
- An expanding region of intermediate ABI values (in green) reaching up to 4 km in altitude.

3. Methodology and results

In this section the study of a particular case of Saharan dust is presented for two southeastern Spain locations: PSA and UAL.

Figure 7 shows the evolution of Aerosol Optical Thickness (AOT) at PSA site, where the measurements were offered by the AERONET station at 1.5 level for 22nd February.

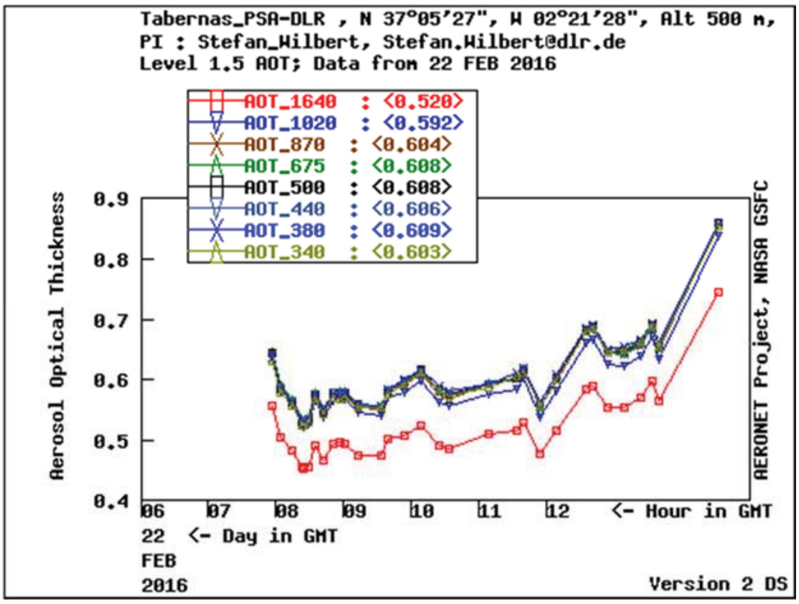

Fig. 7: AERONET AOT at 1.5 level measured at PSA

From the AERONET data, the mean daily value for the Angström turbidity parameter was $\beta \sim 0.6$, indicating an important load of coarse mode aerosols. According to Fig. 7, the AOT values showed an increasing trend along the day.

After that, the first goal was to determine the Linke Turbidity (T_L) under these particular sky conditions. Subsequently, the ESRA clear sky model (Rigollier et al., 2000) was used to obtain a representative T_L factor according to DNI values from PSA. The air mass was set to 2 and the results showed an average T_L of 8.2 (Fig. 8).

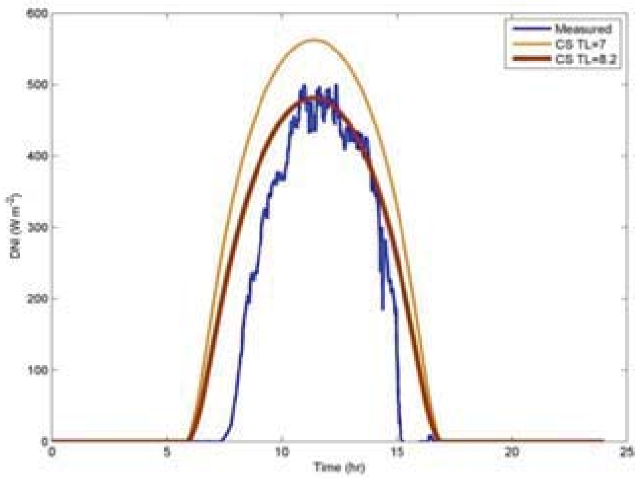

Fig. 8: PSA DNI and ESRA clear sky model using T_L factor of 7 and 8.2 for PSA site on 22nd February 2016

The use of ESRA model for computing Linke turbidity at air mass 2 is required for comparing the results with the estimation of T_L at air mass 2 from the AOT and water vapor using the Ineichen approach (Ineichen, 2008). The estimation of Linke turbidity from inverting the ESRA model is in agreement with the AERONET data. Thus, using the Ineichen model, T_L is computed from AOT and water vapor. AERONET measurements resulted in a mean T_L value of 7. The differences between the estimations of T_L from DNI data and from AERONET are expected taking into account the strong dynamism of the aerosol loading phenomena and the different time stamp between AERONET and pyrheliometer measurements.

Analyzing this factor at UAL emplacement, the estimated T_L was of 10.5, which is an extremely high value. Fig. 9 represents the measured and estimated DNI values using the T_L factor estimate of 10.5.

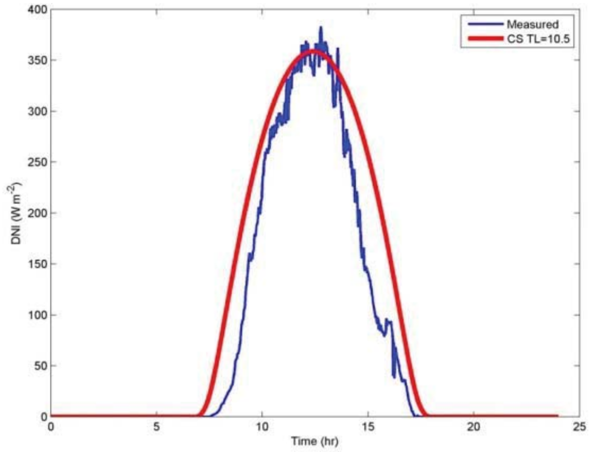

Fig. 9: UAL DNI and ESRA clear sky model using T_L factor of 10.5 for UAL site on 22nd February 2016

3.1 SMARTS simulations

Figure 10 shows the evolution of the AOT at 500 nm and the Angström exponent at (440-675) nm for 4 consecutive days, starting on 22nd February, date where the dust intrusion took place. The AOT values for 22nd February are extremely large, around 0.6, indicating the high aerosol concentration. After two days, the AOT levels diminish to values of about 0.05 corresponding to the clean conditions at the PSA. The atmospheric dust has a large attenuating effect on the solar energy reaching the ground, with a reduction of about 50%. To note, the effect of turbidity is only observed on the first half of the day. In the afternoon, the cloudiness fully blocks DNI, showing values near 0 Wm^{-2}. Besides, the Angström exponent provides useful information about the size distribution of aerosols (Eck et al., 1999). α- values obtained from the spectral band (440-675) nm close to 0 are mainly associated with desert dust. From Fig. 8 it is observed the temporal evolution of α, where zero values appear for the beginning of the dust intrusion increasing until reaching typical values of 1.2-1.3 on 25th February.

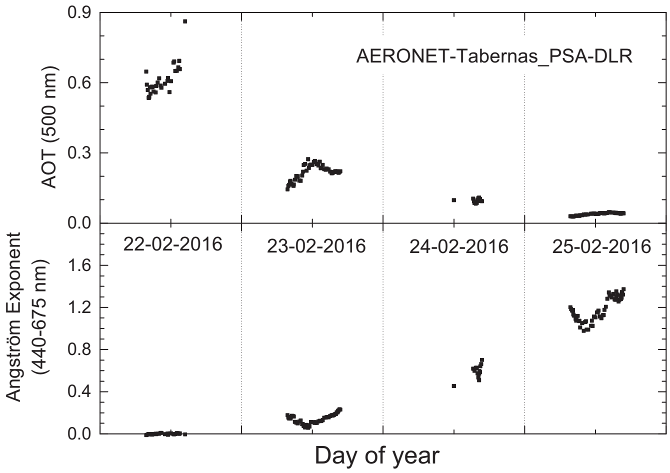

Fig. 10: Time-series of AOT at 500 nm (upper panel) and Angström exponent at (440-675) nm (lower panel) obtained with the AERONET-Cimel at Plataforma Solar de Almería (Spain). Cimel data are AERONET level 1.5 data.

To investigate the type of aerosol, DNI simulations using the SMARTS code (Gueymard, 1995) were carried out. Four different aerosol models available in SMARTS were selected (Tab. 1): the tropospheric aerosol model defined by Shettle and Fenn –"S&F Tropospheric"-, the Maritime aerosol model of the IAMAP preliminary standard atmosphere –"SRA Maritime"-, the "Desert_min" option corresponding to normal conditions in desert areas and "Desert_max" corresponding to extremely turbid conditions.

Tab. 1: Daily mean values of the Angström exponent and the meteorological optical range (MOR) given by SMARTS for the 4 aerosol models considered in this work and corresponding to 22nd February.

Aerosol model	α	MOR (km)
S&F Tropospheric	1.3	14
SRA Maritime	0.24	12
Desert_min	1.13	14
Desert_max	0.0	11

The turbidity coefficient was the AOT (500 nm) given by AERONET. Precipitable water data derived from the sunphotometer (Cimel) was also used. Atmospheric pressure measurements were available from the PSA radiometric station. The atmospheric profile and total column amounts of other atmospheric constituents are those specified by the Mid-Latitude Summer Atmosphere. Tab. 1 shows the daily averaged mean Angström exponent and the Meteorological Optical Range (MOR) obtained from SMARTS for the four aerosol models. The MOR is similar for the four options, however the Angström exponent is different.
The S&F Tropospheric and Desert_min models are not suitable to describe the existing size distribution of aerosols since the values are 1.3 and 1.13 respectively. To compare clear and turbid skies, Fig. 11 shows the DNI measured at PSA for the very turbid day 22nd February and for the day 25th February with the clean atmosphere.

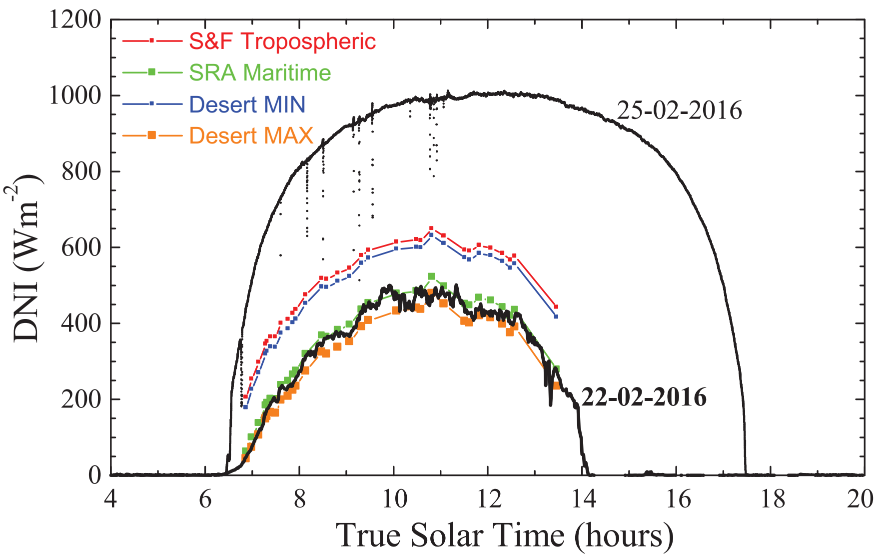

Fig. 11: DNI measured at PSA for the days 22nd February and 25th February (black dots). Simulations using Smarts code corresponding to four different aerosol models are included for the day 22nd February

In addition, the estimated DNI values using the four aerosol types for the 22nd February are also included. The DNI estimates corresponding to the two aerosol models with Angström exponent values close to the measured zero values, i.e. SRA Maritime and Desert_max, show a good agreement with the experimental pyrheliometric measurements. Since the simulated α value corresponding to the Desert_max model matches better the experimental one, this aerosol model is then selected to be representative of the main type of aerosol prevailing in this event.

In the case of UAL site, the Desert_max aerosol model was also used like in PSA site. We also used SMARTS for estimating DNI by using the AOT values derived from the Linke Turbidity factor. Using a MidLat-Summer atmosphere type, and atmospheric pressure and humidity data from the meteorological station placed at UAL, we have checked the influence on the DNI in the aerosol type:

Tab. 2: Cases for the simulation with SMARTS code of the event at UAL.

Aerosol type	AOT (500)	α	MOR (Km)
Desert_max	0.7	0.0	9.4

After obtaining direct normal irradiance values from SMARTS, the model was validated from sunrise to midday, because next to this moment the clouds appeared and SMARTS model works only under cloudless skies.

Estimated and measured values for the complete day are presented in the graph in Fig. 12:

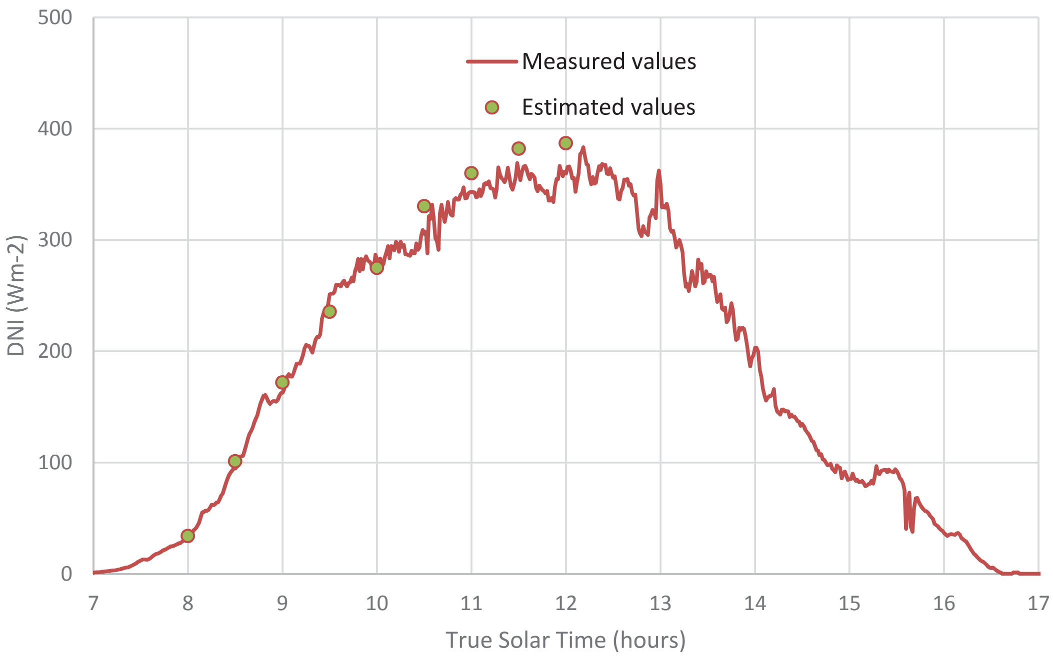

Fig. 12: DNI measured and estimated at UAL using Smarts code

Therefore, estimated DNI values show a good agreement with the measured ones in both cases, having a higher difference at 11:00 and 12:00. In these cases, the estimated values from SMARTS (green dots) presented a higher value than measured values (red line). Mainly, this difference was produced by the appearing of very thin clouds (see Fig. 1); for this reason, the DNI curve presented a different trend from sunrise to midday than from midday to sunset. Due to Saharan dust coming from the south, the saturation was higher at UAL than at PSA.

4. Conclusions

In this work we have made an exhaustive study for 22nd February 2016, with a high presence of dust particles from Sahara desert.
Linke turbidity factor was estimated for PSA and UAL through ESRA clear sky model and the measured DNI data in both sites. In the case of PSA, the best approximation was a TL value of 8.2, whereas for UAL the best value was 10.5, which are expected values for this type of phenomena.
DNI values were analyzed and estimated using SMARTS code by using AOT (500nm) measured at PSA, and desert type aerosols. Subsequently, DNI values were estimated for UAL using the Smarts code, also using desert type aerosols successfully.
In general, we have characterized an episode of turbidity using terrestrial measurements and simulations based on a clear sky radiative transference model in two south-east Spain sites, representing with satisfactory results the type of aerosol which appeared, and accurately modeling the direct normal irradiance during this phenomena. Furthermore, with the correct reproducibility of this extreme episode, the DNI estimation procedure acquires confidence and reliability under this particular sky condition.

Acknowledgments

Financial support by the Education and Competitiveness Ministry of Spain, PRESOL project “Forecast of solar radiation at the receiver of a solar power tower” with references ‘ENE2014-59454-C3-1-R1, 2 and 3’. Also, we thank to the AERONET staff for their support.

5. References

Gueymard, C., *Report 1995. SMARTS2, Simple Model of the Atmospheric Radiative Transfer of Sunshine: Algorithms and Performance Assessment*. Florida Solar Energy Center.

Ineichen, P., 2008. Conversion function between the Linke turbidity and the atmospheric water vapor and aerosol content. Solar Energy 82, 1095–1097. doi:10.1016/j.solener.2008.04.010

Kambezidis, H.D., Paliatsos, A.G., Kappos, N. and Kasselouri, B. 2012. A *Case of African Dust Transport over Athens Captured by a Ceilometer*. In Advances in Meteorology, Climatology and Atmospheric Physics, Springer Atmospheric Sciences, # Springer-Verlag Berlin Heidelberg, 1011-1018.

Rigollier, C., Bauer, O., Wald, L., 2000. On the clear sky model of the ESRA - European Solar Radiation Atlas - with respect to the heliosat method. Solar Energy 68, 33–48. Doi: 10.1016/S0038-092X(99)00055-9